Physics Procedia

Volume 75, 2015, Pages 1314–1323

20th International Conference on Magnetism

Effect of Milling Conditions on the Microstructure and Interphase Exchange Coupling of $Nd_2Fe_{14}B$/α-Fe Nanocomposites

Sever Mican[1], Răzvan Hirian[1], Olivier Isnard[2], Ionel Chicinaş[3], Viorel Pop[1*]

[1]Faculty of Physics, Babeş-Bolyai University, Cluj-Napoca, RO-400084 Romania
[2]Institut Néel, CNRS, Université Grenoble Alpes, BP 166X, 38042 Grenoble, Cédex 9, France
[3]Materials Science and Engineering Department, Technical University of Cluj-Napoca, Cluj-Napoca, RO-400641 Romania

Abstract

The effects of milling conditions on the microstructure and interphase exchange coupling of $Nd_2Fe_{14}B$+10 wt% α-Fe nanocomposites were investigated. The α-Fe crystallite size is critical for obtaining an efficient interphase exchange coupling. The problem of damaging the $Nd_2Fe_{14}B$ crystal structure during milling was addressed by using different milling conditions. $Nd_2Fe_{14}B$+ 10 wt% α-Fe powder samples were prepared through mechanical milling for 6 h with Ø = 10 mm and Ø = 15 mm balls respectively. The restoration of the $Nd_2Fe_{14}B$ crystal structure after annealing was confirmed by XRD, with a limited growth of α-Fe crystallites. The magnetic behavior was investigated from hysteresis curves and dM/dH vs. H plots. The samples milled with small balls show a good interphase exchange coupling, however, milling with larger diameter balls determined higher coercivities due to the reduced damaging of the $Nd_2Fe_{14}B$ crystal structure during milling. The best exchange coupling was obtained for the samples annealed at 750 °C for 1.5 minutes, with a maximum coercive field of about 0.65 T. The $Nd_2Fe_{14}B$ /α-Fe exchange coupling was analyzed as a function of milling and annealing conditions.

Keywords: Soft/hard magnetic nanocomposites, interphase exchange coupling, ball milling, short time annealing.

* Corresponding author: viorel.pop@phys.ubbcluj.ro

 Selection and peer-review under responsibility of the Scientific Programme Committee of ICM 2015

doi:10.1016/j.phpro.2015.12.147

1 Introduction

Today, permanent magnets have become crucial in a wide range of applications, most notably advanced portable electronics and green solutions, such as electric cars and wind turbines [1], [2]. The increasing demand for high performance permanent magnets and the market considerations has opened several research avenues, for instance high performance rare earth free permanent magnets [3] or soft/hard magnetic nanocomposites (spring magnets) [4]. Soft/hard magnetic nanocomposites are comprised of a fine mixture of exchange coupled hard and soft magnetic phases, ensuring high coercivity, high remanence, and potentially very competitive magnets, when comparing the energy product with current commercial products [5]. The $Nd_2Fe_{14}B$/α-Fe spring magnet is interesting not only because of its possible applications, but also from a fundamental research point of view [1], [2], [6]. When compared to the current generation of high performance rare-earth based permanent magnets, soft/hard magnetic nanocomposites could present such advantages as increased thermal stability [7], [8] and higher corrosion resistance [9], in addition to the increased remanence gained through the addition of the soft magnetic phase. Though the list of advantages of such materials is impressive, the challenges involved in producing the nanocomposites are equally great. In order to ensure a strong soft/hard interphase exchange magnetic coupling, the soft magnetic phase crystallites cannot exceed twice the width of the magnetic domain wall of the hard phase, the hard phase must maintain its crystallinity and the entire sample must present a homogeneous microstructure [1], [2], [5], [6]. So far a number of techniques have been used to obtain soft/hard nanocomposites, such as: melt-spinning [10], mechanical milling [11], hot pressing [12] and thin film deposition [13], followed by various annealing procedures.

The structure and magnetic properties of 6 h mechanically milled (MM) nanocomposites $Nd_2Fe_{14}B$/α-Fe were previously studied. After milling, the samples showed poor crystallinity and high defect density. It was shown that the crystallinity of the hard magnetic phase can be restored through short time heat treatment at high temperature, thus limiting the growth of the soft phase crystallites [14]. Previous Scanning Electron Microscopy (SEM) measurements have shown that nanocomposite samples become homogeneous only after 6 h MM [15], therefore it is important to manage the milling conditions employed for that duration of time. It was suggested that higher diameter balls will lead to less pronounced amorphisation of the milled phases [16]. For the above reasons, in this work we investigate the effect of different milling conditions (milling with different diameter balls) on the structural, microstructural and magnetic properties of $Nd_2Fe_{14}B$/10wt%Fe nanocomposites.

2 Experimental details

The $Nd_2Fe_{14}B$ ingot was prepared by induction melting in a purified Ar atmosphere, followed by annealing in vacuum at 950 °C for 72 h. The ingot was crushed and the resulting powder was sieved through a 500 μm sieve. The starting material for the soft magnetic phases was commercial NC 100.24 Fe powder (Höganäs product) below 40 μm. The sieved $Nd_2Fe_{14}B$ powder was mixed with the Fe powder in a weight ratio of 90% $Nd_2Fe_{14}B$/10% Fe. The mixtures were dry-milled under Ar using Ø = 10 mm and Ø = 15 mm diameter balls for 2, 4 and 6 h. The milling vials (with a volume of 80 ml) and balls were made of 440C hardened steel. The ratio between the rotation speed of the disk and the relative rotation speed of the vials was Ω/ω=333/900 rpm with a ball-to-powder weight ratio of 10:1. The samples of milled powder were wrapped in tantalum foil, sealed in quartz tubes and annealed in an inert Ar atmosphere using a preheated furnace at 700, 750 and 800 °C for times ranging from 0.5 to 2.5 minutes. After annealing, the sealed samples were quenched in water. The structure and microstructure of the nanocomposites were investigated using a Bruker D8 Advance X-ray diffractometer using Cu-Kα radiation and Bragg-Brentano focusing geometry. The X-ray diffraction measurements were performed on powder samples using the θ−2θ scan. The mean crystallite size of

α-Fe (±2 nm) and $Nd_2Fe_{14}B$ (±10 nm) were determined from the full width at half maximum (FWHM) values of the (211) diffraction peak of α-Fe at 2θ = 82.3° and the (214) peak of $Nd_2Fe_{14}B$ at 2θ = 37.3° using Scherrer's formula [17]. The FWHM values were obtained by fitting the peaks using a normalized pseudo-Voigt function. For the calculation of the average crystallite size, the instrumental contribution to the peak width was subtracted from the obtained FWHM values. The instrumental broadening was measured from the X-ray diffraction pattern of a reference sample. Because the evaluations were made on annealed samples, the influence of internal stress on the FWHM was neglected. Scanning electron microscopy (SEM) and X-ray microanalysis studies were performed on a Jeol-JSM 5600 LV microscope equipped with an energy dispersive X-ray EDX spectrometer (Oxford Instruments Inca 200 software). For magnetic measurements, the powder samples were blocked in epoxy resin. The demagnetization curves were recorded at room temperature using the extraction method in applied fields up to 10 T [18]. Considering isolated spherical magnetic particles we used a demagnetization factor of 1/3 for the magnetic data and for the calculation of the internal field, H_{int}.

3 Results and Discussions

In order to study the influence of the grinding medium, i.e. geometry and energy of milling, on the microstructure and magnetic properties of $Nd_2Fe_{14}B$+10 wt% Fe nanocomposites, we prepared $Nd_2Fe_{14}B$ samples milled with different diameter balls (Ø = 10 mm and Ø = 15 mm diameter balls

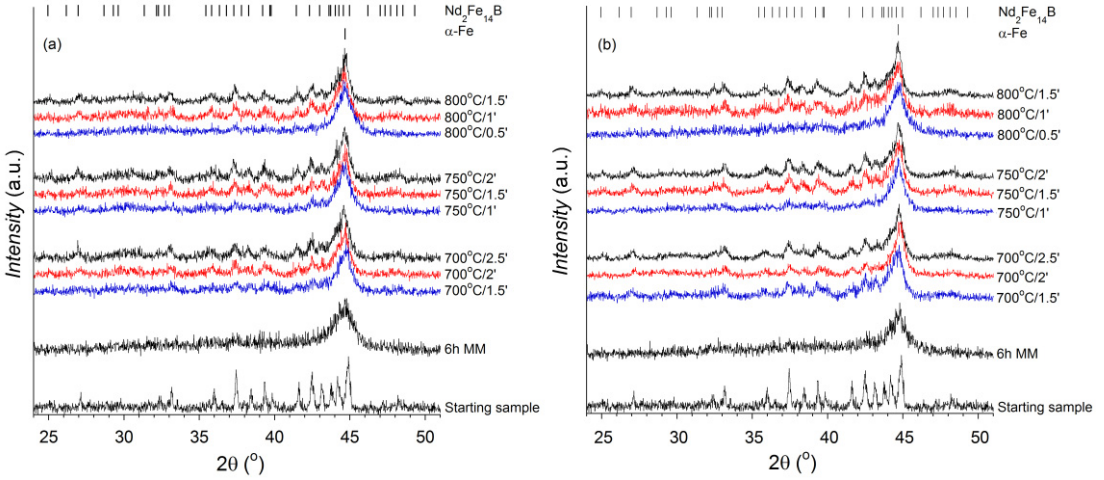

Figure 1: Normalized XRD patterns for the 6 h MM as-milled and annealed $Nd_2Fe_{14}B$+10 wt% α-Fe samples, milled with Ø = 10 mm (a) and Ø = 15 mm (b) balls. For clarity the patterns are shifted vertically.

respectively). The X-Ray diffraction (XRD) patterns for both milled samples, Figure 1, show a broadening of the α-Fe peaks and the $Nd_2Fe_{14}B$ peaks completely disappear after 6h MM, denoting the destruction of the hard phase crystalline structure during milling. After annealing, the XRD peaks of the hard magnetic phase are restored, pointing to the recrystallization of the $Nd_2Fe_{14}B$ phase. It is worthwhile to note that for the annealed samples milled with Ø = 15 mm balls the XRD peaks corresponding to $Nd_2Fe_{14}B$ are more intense and better resolved compared to the same samples milled with Ø = 10mm balls, pointing to a better recrystallization of the hard phase. The FWHM of the (211) peaks of the α-Fe decreases with annealing time and temperature - Figure 2 - pointing to an increase of the α-Fe crystallites. This result is shown more clearly in Figure 3 (a), the average α-Fe crystallite sizes increasing with annealing time and temperature. The average size of the $Nd_2Fe_{14}B$ crystallites - Figure 3 (b) - varies slowly with annealing time for an annealing temperature of 700 ºC, however for

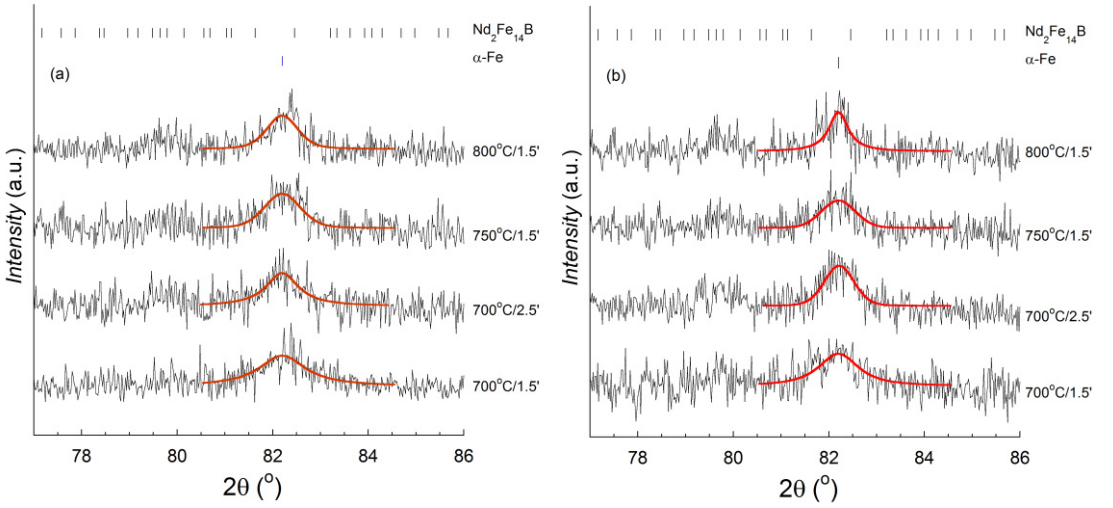

Figure 2 : XRD patterns of the (211) α-Fe peaks for some of the best 6h MM annealed samples milled with balls having a diameter of Ø = 10 mm (a) and Ø = 15 mm (b). For clarity the patterns are shifted vertically.

the samples annealed at 800 ºC, the crystallite sizes show a large increase with annealing time. This could be explained by the fact that $Nd_2Fe_{14}B$ has a recrystallization temperature around 700 ºC [14]. For all annealing conditions, the mean crystallite size is systematically lower when the balls with Ø = 10 mm are used. However, the α-Fe crystallite size values remain in the 5-25 nm range after annealing, showing that the excess growth of the Fe crystallites was hampered during short time annealing.

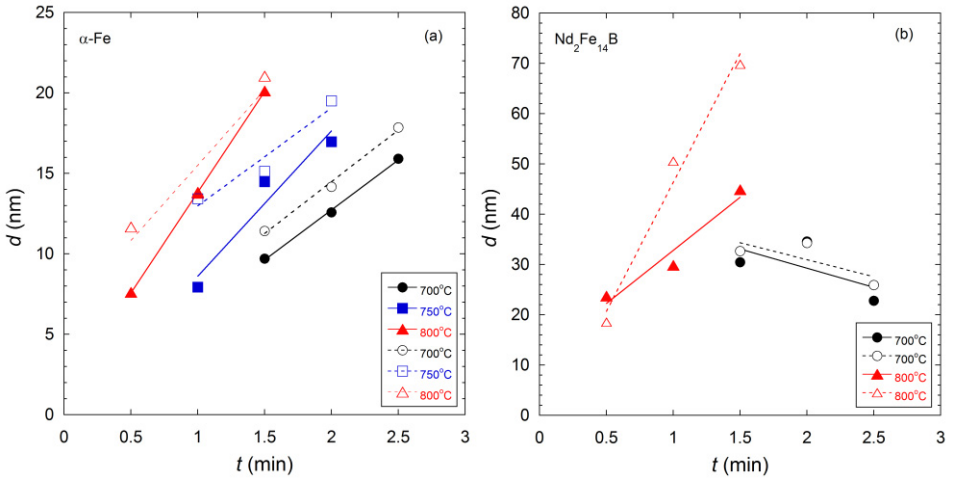

Figure 3: The mean crystallite sizes vs. annealing time for α-Fe (a) and $Nd_2Fe_{14}B$ (b) at the indicated temperature as derived from XRD for the annealed samples milled with Ø = 10 mm (filled symbols) and Ø = 15 mm (empty symbols) balls respectively. The lines are guide for the eye.

The results of the SEM-EDX investigations are shown in Figure 4. The powder particles - Figure 4 top - are comprised of agglomerations of nanoparticles which is a characteristic of milled powders. It can be seen that the grains have an isotropic shape with sizes ranging from several hundred

nanometers to several micrometers. Therefore, for the demagnetizing field correction we considered spherical particles, using a demagnetization factor of 1/3. The EDX analysis of the samples - Figure 4 bottom - shows that the annealed powders are homogeneous, the distributions of Nd and Fe being identical. Previous EDX investigations performed on similar samples [19] showed that the large and small grains present in the SEM images have the same chemical composition proving a good mixing of the hard and soft magnetic nanocrystallites.

The demagnetization curves, after magnetization at 10 T, of the as-milled and annealed samples are shown in Figure 5. Both of the as-milled samples (milled with Ø = 10 mm and Ø = 15 mm balls respectively) show very low coercivity and remanence values - insets of Figure 5 (a),(b) - these samples being comprised mainly of α-Fe and an amorphous matrix resulting from milling [20]. This is consistent with the XRD results, the as-milled samples showing only a wide α-Fe peak - Figure 1. The shape of the demagnetization curves of the annealed samples show a single phase magnetic behavior, except for the sample milled with Ø = 10 mm and annealed at 700 °C for 1.5 min which presents an inefficient coupling. The inefficient coupling shown by this sample could be explained by the fact that the hard magnetic phase is not completely recrystallized after annealing, in good agreement with XRD data from Figure 1 (a). The samples milled with larger diameter balls (Ø = 15 mm) show better magnetic properties, i. e. higher remanence and coercivity than the samples milled with Ø = 10 mm

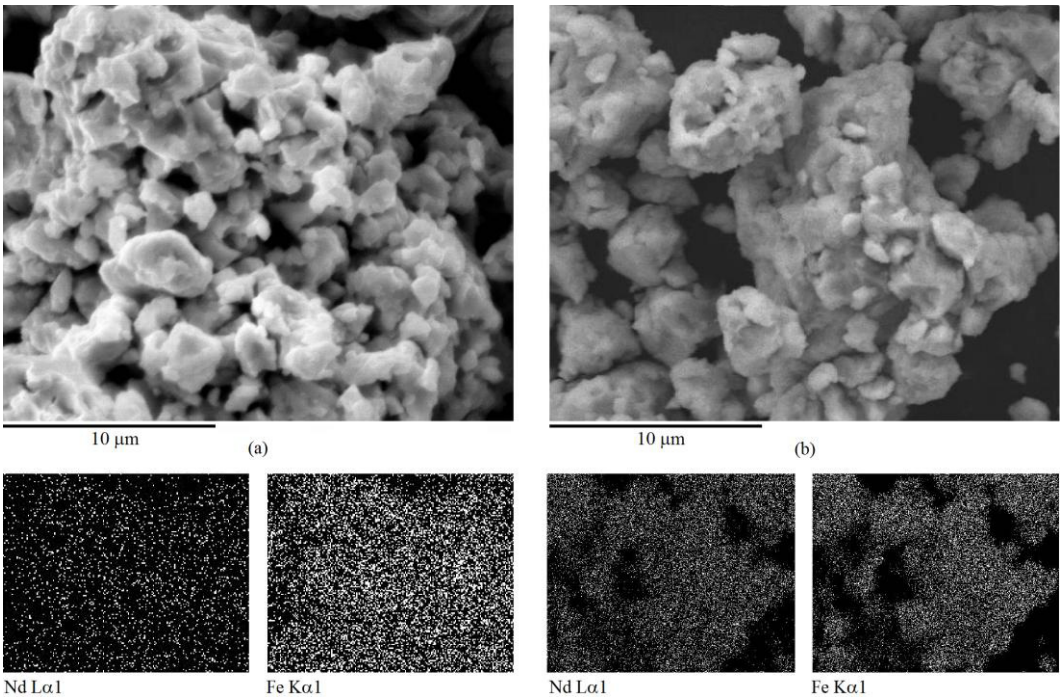

Figure 4: SEM image (top) and EDX analysis (bottom) of the same area for Nd and Fe for:
(a) $Nd_2Fe_{14}B$+ 10wt% α-Fe 6h MM + 750 °C/2' (Ø = 10 mm balls) and
(b) $Nd_2Fe_{14}B$+10 wt% α-Fe 6h MM + 700 °C/1.5' (Ø = 15 mm balls).

balls. This behavior could be attributed to the reduced amorphisation of the hard phase during milling [16], which leads to a better recrystallization after annealing. The dM/dH vs. H plots of the annealed samples are shown in Figure 6. These plots show two peaks, one at low field values around 0.2 T and the other centered between 0.5 - 0.7 T. The dM/dH peak at low fields could correspond to badly coupled or uncoupled Fe and $Nd_2Fe_{14}B$ crystallites, while the peak at higher fields could be attributed

to the exchange coupled nanocomposite. For the sample milled with Ø = 10 mm balls and annealed at 700 °C for 1.5 min the dM/dH vs. H curves show an intense peak at low magnetic field values, confirming the inefficient coupling between the hard and soft phases, while for the samples annealed at higher temperature and/or time the coupling strength increases as pointed out by a significant decrease in the dM/dH peak at low fields, as seen in Figure 6(a). The samples milled with Ø = 15 mm diameter balls show a good interphase coupling for all the samples, indicated by large and rather

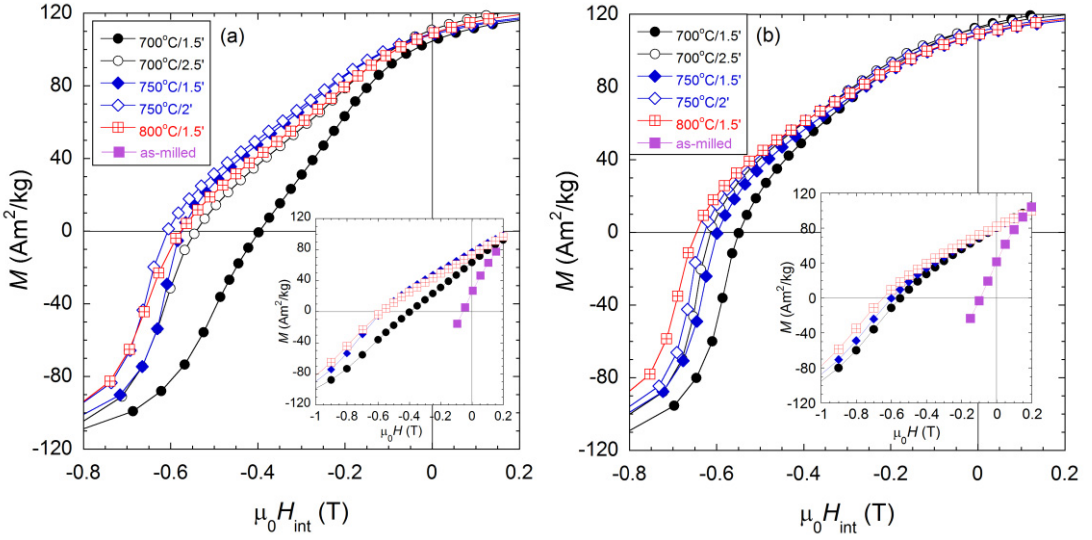

Figure 5: Demagnetization curves for the 6 h MM $Nd_2Fe_{14}B$+10 wt% Fe samples, annealed at the indicated temperatures and times, milled with Ø = 10 mm (a) and Ø = 15 mm (b) balls. The insets show the uncorrected demagnetization curves of the 6 h MM as-milled and annealed samples.

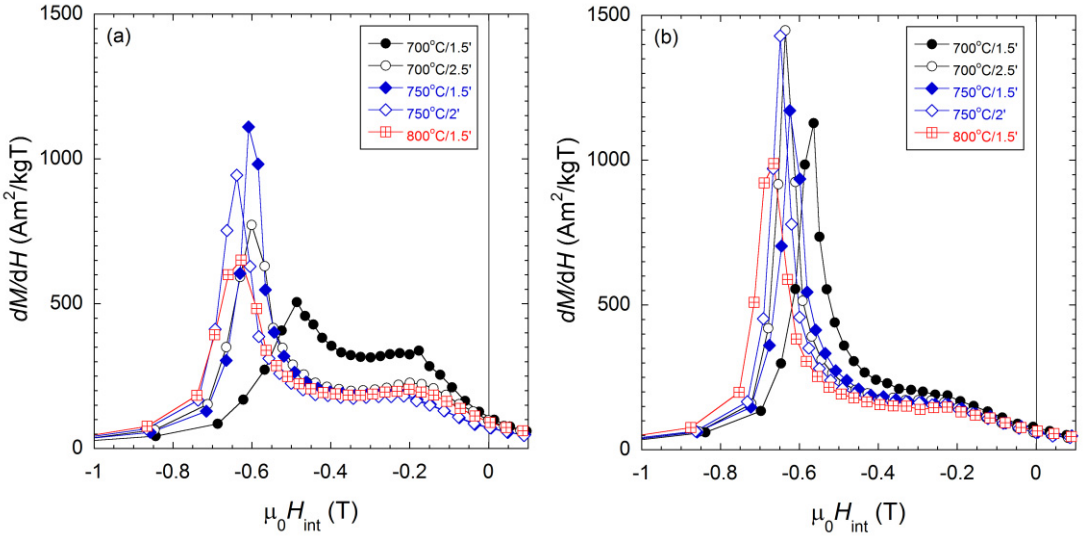

Figure 6: dM/dH versus H curves for the 6 h MM $Nd_2Fe_{14}B$+10 wt% Fe samples, annealed at the indicated temperatures and times, milled with Ø = 10 mm (a) and Ø = 15 mm (b) balls.

narrow peaks at high fields, and a very small peak at low field, Figure 6(b). The better coupling obtained for the samples milled with Ø = 15 mm balls can be explained by the fact that smaller balls (Ø = 10 mm) tend to favor amorphous phase formation [16]. This type of behavior was attributed to intense frictional action favored by milling with smaller balls [16]. Therefore, the structure of the hard magnetic phase is more damaged for the samples milled with Ø = 10 mm diameter balls and more energy is required in order to fully recrystallize the hard phase during annealing. This is most evident in the case of the samples annealed at 700 °C because the temperature is close to the recrystallization temperature of $Nd_2Fe_{14}B$ [14]. This explanation is also backed up by the fact that in this case the Fe crystallites size are similar for both milling types, but the recovery of the hard phase is better when milling with Ø = 15 mm balls, which is confirmed by XRD - Figure 3 (b) - and the magnetic behavior shown in Figure 5.

The coercive field (H_c) and remanent magnetization (M_r) values, determined from demagnetization curves, are summarized in Figure 7 (a) and (b) respectively. For the same annealing conditions, the H_c and M_r values are both higher in the case of larger balls. The coercive field increases with annealing temperature and/or time up to a maximum value of approximately 0.65 T. The higher coercivity values for the samples milled with Ø = 15 mm diameter balls are due to the better interphase exchange coupling between the hard and soft magnetic phases resulting from the better recrystallization of the $Nd_2Fe_{14}B$ phase. It was previously reported that during milling, the $Nd_2Fe_{14}B$ phase can present a

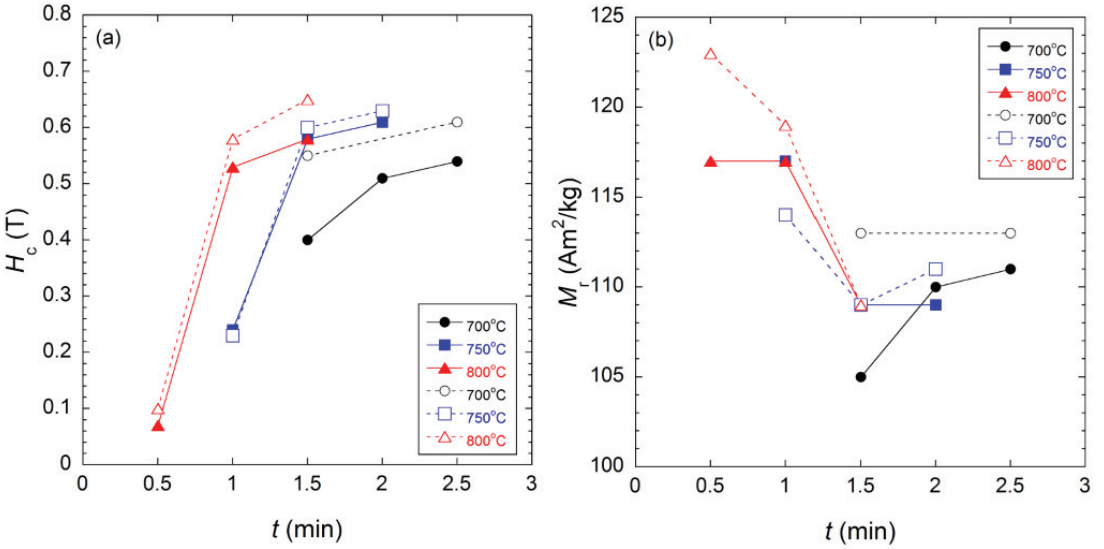

Figure 7: Coercive field (H_c) (a) and remanent magnetization (M_r) (b) vs. annealing time and temperature for the $Nd_2Fe_{14}B$+10 wt% Fe samples milled with Ø = 10 mm (filled symbols) and Ø = 15 mm (empty symbols) balls. The lines are guides for the eye.

separation of Fe from the structure, leading to the formation of Fe crystallites surrounded by an amorphous phase [20]. This causes an increase of the α-Fe phase content in the composite mixture. During annealing, the $Nd_2Fe_{14}B$ phase is progressively restored, meaning that less and less α-Fe, coming from the decomposition of $Nd_2Fe_{14}B$, is present in the powder mixture [20]. This may cause a slight decrease of the remanence values with annealing time, as seen in Figure 7 (b). This assertion is also backed up by the fact that the M_r values for the samples annealed at 750 and 800 °C seem to converge to around 110 Am^2/Kg after 1.5 minutes of annealing. Also, the samples annealed at 700 ºC have lower remanence values than the samples annealed at 750 and 800 °C further proving that the $Nd_2Fe_{14}B$ phase is not fully recovered after annealing at 700 ºC.

The maximum energy product $(BH)_{max}$ is summarized in Figure 8. The $(BH)_{max}$ values increase with annealing time for our samples and slightly increase with annealing temperature. The largest $(BH)_{max}$ values of 185 kJ/m^3 were obtained for samples milled with Ø = 15 mm diameter balls. This value is comparable with other results, on the $Nd_2Fe_{14}B$+Fe system, obtained trough melt spinning, but exceeds the values obtained trough mechanical alloying/milling, for the $SmCo_5$ + Fe system, of 160 and 147 kJ/m^3 respectively [1], [21], [22].

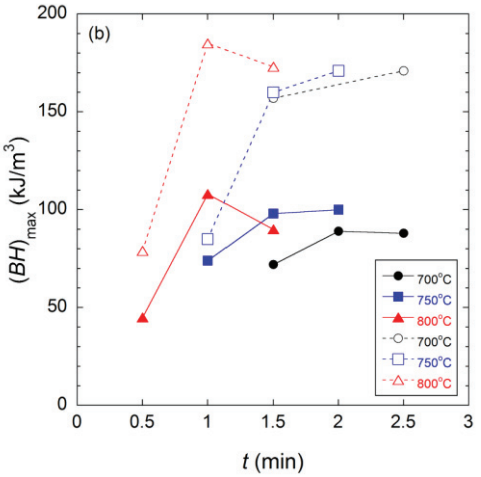

Figure 8: The $(BH)_{max}$ values vs. annealing time and temperature for the $Nd_2Fe_{14}B$+10 wt% Fe samples milled with Ø = 10 mm (filled symbols) and Ø = 15 mm (empty symbols) diameter balls respectively. The lines are guide for the eye.

4 Conclusions

$Nd_2Fe_{14}B$+10 wt% Fe nanocomposites were obtained through ball milling for 6 h using balls of different diameters (Ø = 10 mm and Ø = 15 mm respectively) and subsequent short time annealing at 700, 750 and 800 °C for times ranging between 0.5 and 2.5 minutes, followed by quenching in water. It was shown that the milling conditions and annealing parameters have a significant impact on the structure and microstructure and therefore on the interphase exchange coupling and magnetic properties.

Considering the relations between the coercivity and the crystallinity of the hard magnetic phase, it was shown that milling with larger balls, Ø = 15 mm, have a less destructive effect on the crystal structure of $Nd_2Fe_{14}B$, than milling with the smaller balls, Ø = 10 mm. This result was confirmed by the better resolved XRD peaks corresponding to $Nd_2Fe_{14}B$ and the larger crystallite sizes of the annealed samples milled with Ø = 15 mm balls. Additionally the crystallite sizes of the Fe were small enough, in the 5-20 nm range, to ensure a good hard/soft exchange coupling.

The samples milled for 6 h with larger diameter balls (Ø = 15 mm) showed better magnetic properties (coercive fields of 0.65 T, remanence of 110 Am^2/kg and a high energy product of 185 kJ/m^3) given by a more efficient hard/soft magnetic coupling. This behavior was explained by the less damaged crystallinity of the hard phase after milling, yielding a better crystalline structure recovery after annealing, consistent with the XRD results.

Acknowledgement

The authors would like to acknowledge support from the Romanian UEFISCDI Project No. PN-II-ID-PCE-2012-4-0470.

References:

[1] J. Coey, "Hard Magnetic Materials: A Perspective," *Magnetics, IEEE Transactions on,* vol. 47, no. 12, pp. 4671-4681, Dec 2011.

[2] R. Skomski, P. Manchanda, P. Kumar, B. Balamurugan, A. Kashyap and D. Sellmyer, "Predicting the Future of Permanent-Magnet Materials," *Magnetics, IEEE Transactions on,* vol. 49, no. 7, pp. 3215-3220, July 2013.

[3] M. D. Kuz'min, K. P. Skokov, H. Jian, I. Radulov and O. Gutfleisch, "Towards high-performance permanent magnets without rare earths," *Journal of Physics: Condensed Matter,* vol. 26, no. 6, p. 064205, 2014.

[4] E. Kneller and R. Hawig, "The exchange-spring magnet: a new material principle for permanent magnets," *Magnetics, IEEE Transactions on,* vol. 27, no. 4, pp. 3588-3560, Jul 1991.

[5] R. Skomski and J. M. D. Coey, "Giant energy product in nanostructured two-phase magnets," *Phys. Rev. B,* vol. 48, pp. 15812-15816, Dec 1993.

[6] P. K. Sahota, Y. Liu, R. Skomski, P. Manchanda, R. Zhang, M. Franchin, H. Fangohr, G. C. Hadjipanayis, A. Kashyap and D. J. Sellmyer, "Ultrahard magnetic nanostructures," *Journal of Applied Physics,* vol. 111, no. 7, pp. 07E345, 2012.

[7] D. Goll, M. Seeger and H. Kronmüller, "Magnetic and microstructural properties of nanocrystalline exchange coupled PrFeB permanent magnets," *Journal of Magnetism and Magnetic Materials,* vol. 185, no. 1, pp. 49-60, 1998.

[8] D. Suess, M. Dahlgren, T. Schrefl, R. Grössinger and J. Fidler, "Micromagnetic analysis of remanence and coercivity of nanocrystalline Pr–Fe–B magnets," *Journal of Applied Physics,* vol. 87, no. 9, pp. 6573-6575, 2000.

[9] M. Jurczyk and J. Jakubowicz, "Improved temperature and corrosion behaviour of nanocomposite $Nd_2(Fe,Co,M)_{14}B/\alpha$-Fe magnets," *Journal of Alloys and Compounds,* vol. 311, no. 2, pp. 292-298, 2000.

[10] A. Teplykh, Y. Chukalkin, S. Lee, S. Bogdanov, N. Kudrevatykh, E. Rosenfeld, Y. Skryabin, Y. Choi, A. Andreev and A. Pirogov, "Magnetism of ordered and disordered alloys of $R_2Fe_{14}B$ (R = Nd, Er) type," *Journal of Alloys and Compounds,* vol. 581, pp. 423-430, 2013.

[11] L. Zheng, B. Cui and G. C. Hadjipanayis, "Effect of different surfactants on the formation and morphology of $SmCo_5$ nanoflakes," *Acta Materialia,* vol. 59, no. 17, pp. 6772-6782, 2011.

[12] H. Kwon, Y. Zhang and G. Hadjipanayis, "Effect of host and added alloy composition on magnetic properties of $Nd_2Fe_{14}B$+$Nd_2Fe_{14}B$/Fe hybrid magnets," *Journal of Magnetism and Magnetic Materials,* vol. 303, no. 2, pp. e410 - e414, 2006.

[13] V. Neu, S. Sawatzki, M. Kopte, C. Mickel and L. Schultz, "Fully Epitaxial, Exchange Coupled $SmCo_5$/Fe Multilayers With Energy Densities above 400 kJ/m^3," *Magnetics, IEEE Transactions on,* vol. 48, no. 11, pp. 3599-3602, Nov 2012.

[14] V. Pop, S. Gutoiu, E. Dorolti, O. Isnard and I. Chicinaş, "The influence of short time heat treatment on the structural and magnetic behaviour of $Nd_2Fe_{14}B/\alpha$-Fe nanocomposite obtained by

mechanical milling," *Journal of Alloys and Compounds,* vol. 509, no. 41, pp. 9964-9969, 2011.

[15] V. Pop, O. Isnard, I. Chicinaş, D. Givord and J. M. L. Breton, "$SmCo_5$/α-Fe nanocomposite material obtained by mechanical milling and annealing," *Journal of optoelectronics and advanced materials,* vol. 8, no. 2, pp. 494-500, 2006.

[16] C. Suryanarayana, "Mechanical alloying and milling," *Progress in Materials Science,* vol. 46, pp. 1-186, 2001.

[17] P. Scherrer, "Bestimmung der Grosse und der inneren Struktur von Kolloidteilchen mittels Rontgensrahlen," *Gttinger Nachrichten Gesell,* vol. 2, pp. 98-100, 1918.

[18] A. Barlet, J. Genna and P. Lethuillier, "Insert for regulating temperatures between 2 and 1000 K in a liquid helium dewar: Description and cryogenic analysis," *Cryogenics* , vol. 31, no. 9, pp. 801-805, 1991.

[19] S. Gutoiu, O. Isnard, I. Chicinaş, F. Popa, A. Takacs and V. Pop, "The influence of milling and annealing conditions on the structural and magnetic behavior of $Nd_2Fe_{14}B$/a-Fe hard/soft magnetic nanocomposites," *Journal of Alloys and Compounds,* vol. 646, pp. 859-865, 2015.

[20] T. Alonso, H. Yang, Y. Liu and P. G. McCormick, "De-mixing of $Nd_2Fe_{14}B$ during mechanical milling," *Applied Physics Letters,* vol. 60, pp. 833-834, 1992.

[21] J. Zhang, S.-y. Zhang, H.-w. Zhang and B.-g. Shen, "Structure, magnetic properties, and coercivity mechanism of nanocomposite $SmCo_5$/α-Fe magnets prepared by mechanical milling," *Journal of Applied Physics,* vol. 89, no. 10, pp. 5601-5605, 2001.

[22] A. M. Gabay, G. C. Hadjipanayis, M. Marinescu and J. F. Liu, "Hot-deformed Sm–Co/Co composite magnets fabricated from powder blends," *Journal of Applied Physics,* vol. 107, no. 9, pp. 09A704, 2010.